



Check for updates

## METHOD ARTICLE

# Interactive visualization of spatial omics neighborhoods

[version 1; peer review: 2 approved with reservations]

Tinghui Xu , Kris Sankaran

Department of Statistics, University of Wisconsin-Madison, Madison, Wisconsin, 53706, USA

**V1** First published: 18 Jul 2022, 11:799  
<https://doi.org/10.12688/f1000research.122113.1>Latest published: 18 Jul 2022, 11:799  
<https://doi.org/10.12688/f1000research.122113.1>

## Abstract

Dimensionality reduction of spatial omic data can reveal shared, spatially structured patterns of expression across a collection of genomic features. We studied strategies for discovering and interactively visualizing low-dimensional structure in spatial omic data based on the construction of neighborhood features. We designed quantile and network-based spatial features that result in spatially consistent embeddings. A simulation compares embeddings made with and without neighborhood-based featurization, and a re-analysis of Keren *et al.*, 2019 illustrates the overall workflow. We provide an R package, NBFvis, to support computation and interactive visualization for the proposed dimensionality reduction approach. Code and data for reproducing experiments and analysis are available on [GitHub](#).

## Keywords

Spatial Omics, Interactive Visualization, Dimensionality Reduction, Networks



This article is included in the [Bioinformatics gateway](#).

## Open Peer Review

### Approval Status ? ?

	1	2
<b>version 1</b>		
18 Jul 2022	<a href="#">view</a>	<a href="#">view</a>

1. **Guangdun Peng** , University of Chinese Academy of Sciences, Center for Cell Lineage and Atlas, Bioland Laboratory, Guangdong Provincial Key Laboratory of Stem Cell and Regenerative Medicine, Guangzhou Institutes of Biomedicine and Health, Guangzhou, China  
**Miao Zhu**, GIBH, CAS, Guangzhou, China
2. **Oscar Ospina**, Moffitt Cancer Center, Tampa, USA

Any reports and responses or comments on the article can be found at the end of the article.

**Corresponding authors:** Tinghui Xu ([txu98@wisc.edu](mailto:txu98@wisc.edu)), Kris Sankaran ([ksankaran@wisc.edu](mailto:ksankaran@wisc.edu))

**Author roles:** **Xu T:** Conceptualization, Methodology, Software, Visualization, Writing – Original Draft Preparation, Writing – Review & Editing; **Sankaran K:** Conceptualization, Methodology, Supervision, Visualization, Writing – Original Draft Preparation, Writing – Review & Editing

**Competing interests:** No competing interests were disclosed.

**Grant information:** The author(s) declared that no grants were involved in supporting this work.

**Copyright:** © 2022 Xu T and Sankaran K. This is an open access article distributed under the terms of the [Creative Commons Attribution License](#), which permits unrestricted use, distribution, and reproduction in any medium, provided the original work is properly cited.

**How to cite this article:** Xu T and Sankaran K. **Interactive visualization of spatial omics neighborhoods [version 1; peer review: 2 approved with reservations]** F1000Research 2022, 11:799 <https://doi.org/10.12688/f1000research.122113.1>

**First published:** 18 Jul 2022, 11:799 <https://doi.org/10.12688/f1000research.122113.1>

## Introduction

Spatially resolved omics technologies provide a view into the landscape of complex biological processes (Burgess, 2019; Nawy, 2018). For example, they have revealed novel aspects of tissue differentiation and the structure of certain cancers (Rao et al., 2021; Yoosuf et al., 2020). A spatial transcriptomic or proteomic dataset can be viewed as a spatially indexed collection of high-dimensional vectors (Dries et al., 2021a). The coordinates of each vector correspond to different genomic features (genes expression and protein measurements for spatial transcriptomics and proteomics, respectively) while the spatial index locates each measurement at some location in a tissue or cell.

Two challenges in the analysis of spatial omics data are:

- Microenvironment dimensionality reduction: considering the large number of simultaneously measured genomic features, some form of dimensionality reduction is essential for effective exploratory analysis. However, for spatially resolved data, a dimensionality reduction should describe microenvironments and their relationships with one another. It is more useful to embed the genomics signature of a cell's local neighborhood than simply the cell in isolation.
- Streamlined navigation: low-dimensional representations of microenvironments may not be interpretable on their own. To this end, it is helpful to relate the representations to their original spatial and genomic contexts. Ensuring that these correspondences can be explored efficiently is a challenge in itself.

This paper discusses methods to address these challenges and releases a new R package that implements them. For the first challenge, our approach was to featurize spatial neighborhoods and pass this representation to downstream dimensionality reduction techniques. We explored in-depth features based on (1) histograms of expression levels and (2) local cell network properties. For the second challenge, we designed an interactive visualization that links learned representations with contextual descriptors.

We evaluated these methods using simulation and a qualitative data analysis. The simulation clarifies the difference between learning representations on individual cells and local cellular neighborhoods. The data analysis recapitulates the findings of (Chen et al., 2020; Keren et al., 2019). We believe that the main advantages of the proposed approach are:

- Modularity: the approach can be made use of existing dimensionality-reduction methods while ensuring that results reflect meaningful spatial structure.
- Flexibility: spatial featurizations can be tailored to specific problem contexts with little changes to the overall workflow.

Our methods are implemented in the R package NBFvis, available on [GitHub](#).

The remainder of the paper is organized as follows. The Background subsection reviews relevant literature on analysis of spatial omic data. The Methods section describes the proposed method. The Visualisation subsection introduces what kinds of visualization and interactivity are provided in our package. The Simulation subsection and the Results section illustrate the method in simulation and real data analysis, respectively. The Package subsection gives an overview of NBFvis's functionality. We conclude with a summary and directions for future work in the Discussion.

## Background

The proliferation of spatial omic data has attracted attention from the modeling and visualization communities. Important themes that have emerged include the selection of spatially varying genes, derivation of spatial summary measures, and discovery of spatially consistent microenvironments. The resulting software packages allow analysts to generate overviews of spatial variation as well as focus on specific genomic features of interest.

Several studies propose feature-level models of spatial variation to select those with notable spatial expression patterns. SPARK fits a collection of random effects models with diverse sets of kernels to capture variation at several spatial scales Sun et al. (2020). Alternatively (Zhu and Sabatti, 2020), computed a measure of spatial variation based on a spatially induced graph laplacian; genes exhibiting similar patterns of spatial expression are then clustered. Alternatively (Hsu and Culhane, 2020), proposed an adaptation of Moran's *I*-statistic to measure the extent of spatial clustering across cell types, highlighting the potential for the classical spatial statistics methods to support modern spatial omics analysis. Like NBFvis, these methods compute spatial statistics to summarize spatial omics datasets. However, they tend not to provide localized measures of spatial structure, focusing instead on tissue-level properties.

The Giotto package includes approaches to dimensionality reduction and interactive visualization of spatial omics data [Dries et al. \(2021b\)](#). Of particular interest, the package supports interactive visualization that dynamically links embeddings of expression measurements with corresponding cell locations. Note however that these embeddings are derived without reference to spatial features.

Similar to our approach, Spatial-LDA proposes a variation of the topic models that learns spatially consistent patterns of cell type mixing ([Chen et al., 2020](#)). This is achieved by tying together mixed memberships of neighboring cells in a structured prior, and the model is fitted using a custom optimization scheme. Regions with similar topic memberships can be interpreted as microenvironments. Our proposal has a similar data analytic goal; however, we aim to support more generic spatial features while preserving simplicity in implementation.

### Simulation

We provided a toy simulation to clarify the differences in embeddings when neighborhood information is and is not used. We found that if only cell-level information is considered, the embeddings will be dominated by cell types and fail to reflect microenvironment structure.

### Dataset construction

Assume that there is one tissue section with three cell types. For each cell, five proteins are measured. Different cell types have different protein profiles, which means the average measurements of proteins differ according to cell type. We assume that cell types are clustered spatially, but that these clusters are close enough so that some areas overlap. These overlapping areas can be considered different microenvironments since the local mixture of protein profiles is different from regions of pure cell types.

**Figure 1** is the spatial plot for the simulated dataset. Two thousand “cells” are generated and divided into three different cell types according to a multinomial distribution with the probability (0.2, 0.3, 0.5) for Cell Type 1, 2, and 3,

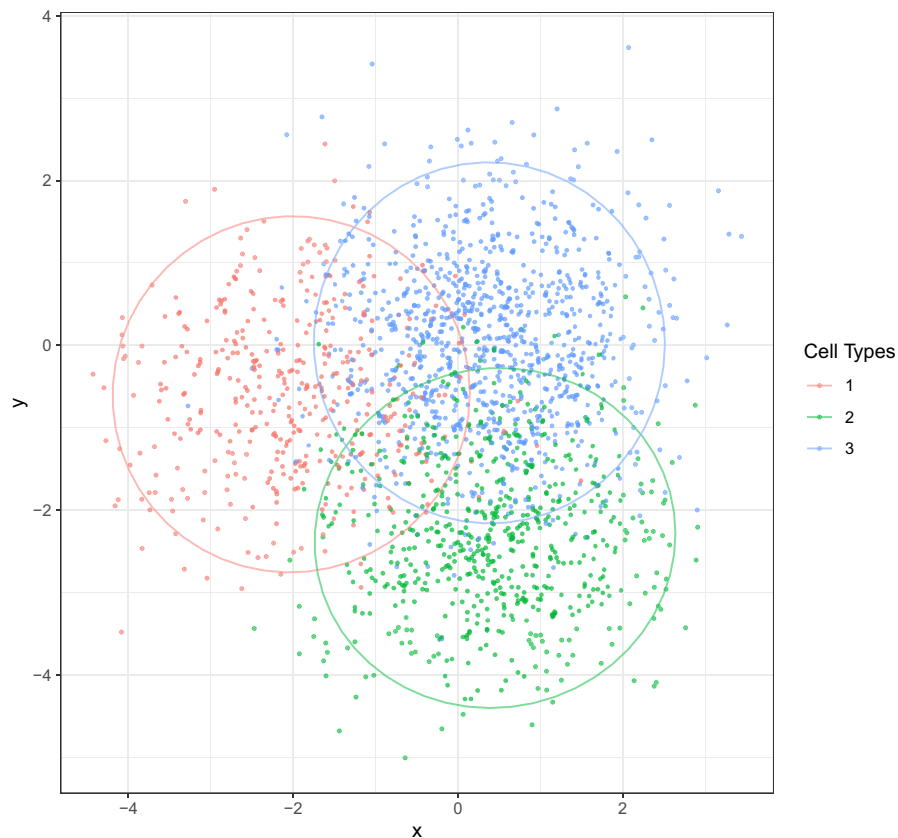


**Figure 1. Simulation of a tissue section with three different, partially overlapping cell types.** Overlapping regions can be thought of as their distinct microenvironments. The goal is to construct embeddings that reflect different mixing patterns.

$$c_i \sim \text{Mult}(1, (0.2, 0.3, 0.5)), i = 1, \dots, 2000,$$

where  $c_i$  is the cell type of the  $i^{\text{th}}$  cell.

For this demonstration, we imagined that protein abundances are drawn from a mixture of multivariate normals. The average of each mixture component represents the typical cell profile for each cell type. That is, for each cell, the measurements for each of the five proteins have the form,

$$p_i | \mu_{c_i} \sim \mathcal{N}(\mu_{c_i}, 5I_5), i = 1, \dots, 2000$$

$$\mu_j \sim \mathcal{N}(0, 8I_5), j = 1, 2, 3,$$

where  $\mu_j$  is the average protein profile for the  $j^{\text{th}}$  cell type and  $p_i$  is a five-dimensional measurement for the  $i^{\text{th}}$  cell.

Next, we simulated cell locations to get mixed spatial patterns. We used a different mixture of (now two-dimensional) multivariate normals. As before, component means  $\text{center}_1$ ,  $\text{center}_2$ , and  $\text{center}_3$  were drawn from a multivariate normal. Denoting the coordinates of cell  $i$  by  $(x_i, y_i)$  and the spatial mean of cell type  $j$  by  $\text{center}_j$ , we drew,

$$(x_i, y_i) | \text{center}_{c_i} \sim \mathcal{N}(\text{center}_{c_i}, 2I_2)$$

$$\text{center}_j \sim \mathcal{N}(0, 10I_2).$$

After simulation, we obtained a  $2000 \times 5$  expression matrix, each row of which corresponds to the simulated observation of one cell. We called this matrix the “single cell matrix”.

To extract neighborhood information for each cell, we first found neighborhoods with a given radius (here we used 0.2 units in length). We then calculated statistics within each neighborhood. We chose quantiles of protein content as neighborhood-based statistics, which are simple but effective. For every cell and protein, we derived 21 quantiles  $q_0, q_{0.05}, \dots, q_1$  in the neighborhood. After calculation, an extended  $2000 \times 105$  matrix was obtained. We called this the “neighborhood matrix”.

### Comparison

We next applied dimensionality reduction methods to both the single cell and the neighborhood matrices, in order to clarify the difference in the resulting embeddings.

First, we applied uniform manifold approximation and projection (UMAP) [McInnes et al. \(2018\)](#) to the single cell matrix, whose low-dimensional embeddings are shown in [Figure 2](#). Only three separate clusters are visible in the embedding plot,

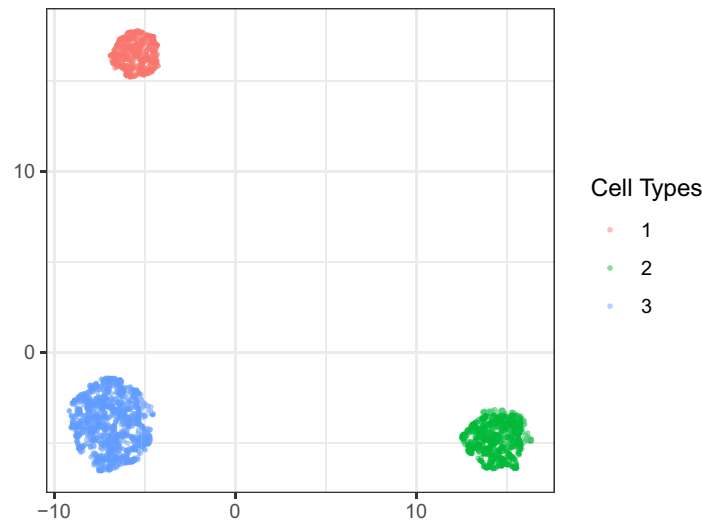


**Figure 2. A UMAP embedding plot on the single cell matrix.** Cell types clustered with one another, but different mixture patterns were not observed. The embeddings were dominated by the cell types, obscuring the presence of microenvironments.

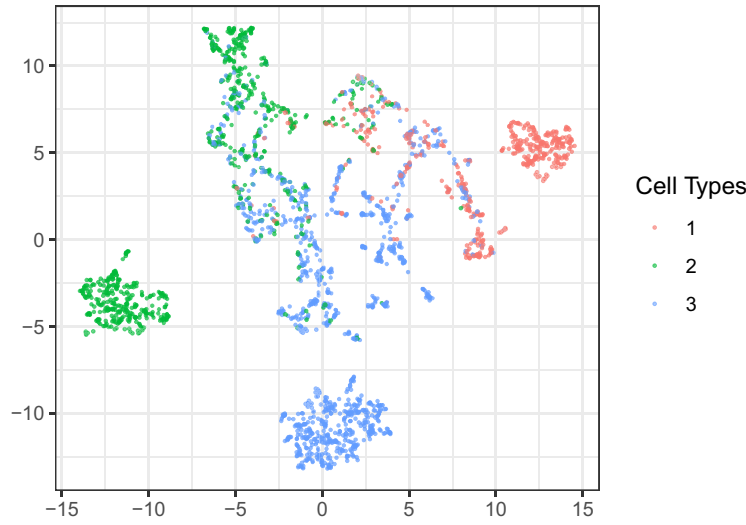


**Figure 3. A UMAP embedding plot on the neighborhood matrix.** Though simple, the neighborhood quantile statistics make it possible to detect mixture microenvironments. We could further find subclusters like the red-green mixture in the central cluster.

each corresponding to a cell type. These UMAP embeddings ignore the microenvironments of mixed cell types along cluster borders in the spatial plot. This result indicates that, when spatial information is not directly incorporated, the low-dimensional embeddings are dominated by cell types and fail to distinguish microenvironments.

In contrast, the embedding plot of the neighborhood matrix detects microenvironment structures; see Figure 3. We noticed that there were still three clusters consisting of pure cell types. However, there were additional clusters of mixed cell types. Between the three pure clusters is a region corresponding to microenvironments with mixed cell types in the spatial plot. Furthermore, we noticed that this region can be further divided into spatially consistent “subclusters”. For instance, one region with only blue and green cells was related to the blue-green spatial boundary. This can be treated as a unique microenvironment. Similar red-blue and red-green regions were also visible.

In summary, UMAP embeddings using the single cell matrix were dominated by cell types and failed to detect microenvironments with mixed cell types. However, by simply applying UMAP to the neighborhood matrix, we were able to detect these spatially meaningful microenvironments.

## Methods

First, we established notation and an overview of the general approach. Let  $X \in \mathbb{R}^{N \times D}$  contain expression measurements for  $D$  gene or protein expression features across  $N$  cells. We call  $X$  the expression matrix. Let  $S \in \mathbb{R}^{N \times 2}$  contain the spatial locations of the  $N$  cells. We first applied a preliminary dimensionality reduction, like principal component analysis (PCA), to the expression matrix  $X$  before the following neighborhood-based featurization. We called the reduced matrix  $\hat{X} \in \mathbb{R}^{N \times P}$ , where  $P$  is the number of dimensions after dimensionality reduction.

Before we can embed properties of cell neighborhoods, we need to define and derive features for each neighborhood. For each cell  $x_i$ , we defined its neighborhood using distances induced by  $S$ , either containing all cells within a certain radius or simply the  $K$ -nearest neighbors. Denote the neighborhood for the cell  $x_i$  by  $m(i) = (x_{(i,1)}, \dots, x_{(i,n_i)})$ , where  $x_{(i,1)}, \dots, x_{(i,n_i)}$  are the  $n_i$  neighbors in the neighborhood and  $n_i$  is the number of neighbors surrounding  $x_i$ . We featurized the neighborhoods  $m(i)$  using neighborhood-based featurization functions  $T_j, j = 1, \dots, J$ . We then rescaled all the derived featurization matrices  $T_1(\hat{X}), T_2(\hat{X}), \dots, T_J(\hat{X})$  and concatenated them to obtain an extended neighborhood-based featurization  $T(X)$ . The neighborhood matrix from the Simulation subsection is a special case of  $T(X)$  using quantile features.

In more detail, let  $T_j: \mathbb{R}^P \rightarrow \mathbb{R}^{p_j}, j = 1, 2, \dots, J$  be a set of featurization functions. By applying every  $T_j(m(i))$  to each neighborhood  $m(i)$ , we can construct  $\tilde{X}_j \in \mathbb{R}^{N \times p_j}$ . The matrix  $\tilde{X}_j$  can be rescaled and then combined into a widened neighborhood matrix  $\tilde{X} \in \mathbb{R}^{N \times \sum_{j=1}^J p_j}$ . This neighborhood matrix  $\tilde{X}$  was input to a dimensionality reduction method to

recover a set of embeddings. Our final set of microenvironments was found by clustering these embeddings. Below, we applied  $K$ -means to the set of neighborhood-level embeddings.

### Example

We next discuss a specific instantiation of this general procedure, describing the neighborhood and featurization choices used in the Results section and implemented in NBFvis. There,  $N$  gives the number of cells in one tissue section,  $D$  is the number of proteins measured, and  $s$  is the spatial location matrix of the segmented cells. We applied a PCA to the expression matrix  $X \in \mathbb{R}^{N \times D}$  and then derived the reduced expression matrix  $\tilde{X} \in \mathbb{R}^{N \times P}$ . Neighborhoods were constructed by keeping the  $K$  nearest neighbors that are also within a given radius.

We used two types of featurization functions  $T_j$  – quantile features and network features. For the  $i^{\text{th}}$  cell’s neighborhood,  $Z$  quantiles  $(q_1^{i,k}, q_2^{i,k}, \dots, q_Z^{i,k})$  were calculated for the  $k^{\text{th}}$  protein, where  $k = 1, 2, \dots, P$ . It means that we derived a  $PZ$ -dimensional vector  $(q_1^{i,1}, q_2^{i,1}, \dots, q_{Z-1}^{i,P}, q_Z^{i,P})$  for each neighborhood. Thus,  $T_{\text{quantile}}(X) : \mathbb{R}^{N \times P} \rightarrow \mathbb{R}^{N \times PZ}$ . After featurization, we obtained an  $N \times PZ$  matrix, which we called the “quantile matrix”. Next, consider the construction of network features. Let  $G_i$  denote the geometric graph associated with  $m_i$ , using the metric induced by  $s$ . Based on  $G_i$ , we can calculate a variety of node or edge features. The associated network featurization here is  $T_{\text{network}}(X) : \mathbb{R}^{N \times P} \rightarrow \mathbb{R}^{N \times M}$ , where  $M$  is the number of network statistics. For example, in the experiments below, we used the number of edges  $\text{degree}(G_i)$  and a variety of centrality measures. We used an ensemble of 29 network-based statistics in our example, detailed in [Table 1](#) and the *Extended Data XTH1114* and [Sankaran \(2022\)](#).

**Table 1. Centrality Table.** We use implementations of these centrality measures from the R packages `igraph` (Csardi and Nepusz, 2006), `centiserve` (Jalili, 2017) and `sna` (Butts, 2020). Network statistics implemented in NBFvis. These functions could be found in `centiserve` and `snr` package.

Name	Description
Number of nodes	The number of nodes in the neighborhoods.
Degree	The number of edges the node has.
Betweenness	The number of shortest paths that pass through the node.
Closeness	The reciprocal of the sum of the length of the shortest paths between the node and all other nodes
Eigencentrality	It measures the influence of a node has in the network. If a node is linked by many nodes with high eigenvector centrality, then that node itself will have high eigenvector centrality.
The reciprocal of eccentricity	The reciprocal of the longest shortest paths from the node to other ones.
Subgraph centrality	It measures the number of subgraphs a node participates in, weighting them according to their size.
Load centrality	The fraction of all shortest paths that pass through that node.
Gil-Schmidt power centrality index	It takes a value of 1 when the node is adjacent to all reachable nodes, and approaches 0 as the distance from the node to each node approaches infinity.
Information centrality scores	It measures the harmonic mean length of paths ending at the node, which is smaller if the node has many short paths connecting it to other nodes.
Stress centrality	If the node has a high stress centrality, it is traversed by a high number of shortest paths.
The reciprocal of average distance	The reciprocal of the average of the shortest paths.
Barycenter centrality	The reciprocal of the total distance from the node to all other nodes.
Variant closeness centrality	The sum of inversed distances to all other nodes.
Residual closeness centrality	The minimum of the closeness centrality of the node when one node is deleted.
Communicability betweenness centrality	If a node $v$ has a low communicability betweenness centrality, there are few shortest paths pass through $v$ among the pairs of nodes.
Cross-clique connectivity	The number of cliques to which belongs.
Decay centrality	The sum of distances between a chosen node and every other node weighted by the decay.

**Table 1.** *Continued*

Name	Description
Diffusion Degree	The cumulative contribution score of the node itself and its neighbors in a diffusion process.
Geodesic 3-path centrality	The number of neighbors on a geodesic path less than 3 away.
Laplacian centrality	The drop in the sum of squares of the eigenvalues in the Laplacian matrix when the node is removed.
Leverage centrality	It measures the relationship between the degree of a given node and the degree of each of its neighbors, averaged over all neighbors.
Lin centrality	It is a weighting closeness for graphs with infinite distances using the square of the number of coreachable nodes.
Lobby centrality	The largest integer $k$ such that $x$ has at least $k$ neighbors with a degree of at least $k$ .
Markov centrality	It uses the mean first-passage time from every node to every other node to produce a centrality score for each node.
Maximum neighborhood component	The size of the maximum connected component of the neighborhood. The neighborhood here is the set of nodes adjacent to the node and does not contain this node.
Radiality centrality	High radiality indicates that the node is generally closer to the other nodes with respect to the diameter. Low radiality means that the node is peripheral.
Semi local centrality	The sum of the number of the nearest and the next nearest neighbors of the nodes who are the nearest neighbors of the given node.
The reciprocal of the topological coefficient	The topological coefficient measures the extent to which a node shares neighbors with other nodes in an undirected graph.

The final featurization combined both quantile and network features,

$$T(\hat{X}) = [T_{\text{quantile}}(\hat{X}), T_{\text{network}}(\hat{X})].$$

$T(X)$  is a  $N \times (PZ + M)$  neighborhood matrix. Rescaling was applied to this neighborhood matrix so that every column was on a similar scale. This rescaled neighborhood matrix was passed to UMAP to obtain low-dimensional embeddings. These embeddings could then be clustered to identify distinct microenvironments. The whole workflow is shown in [Figure 4](#).

### Implementation details

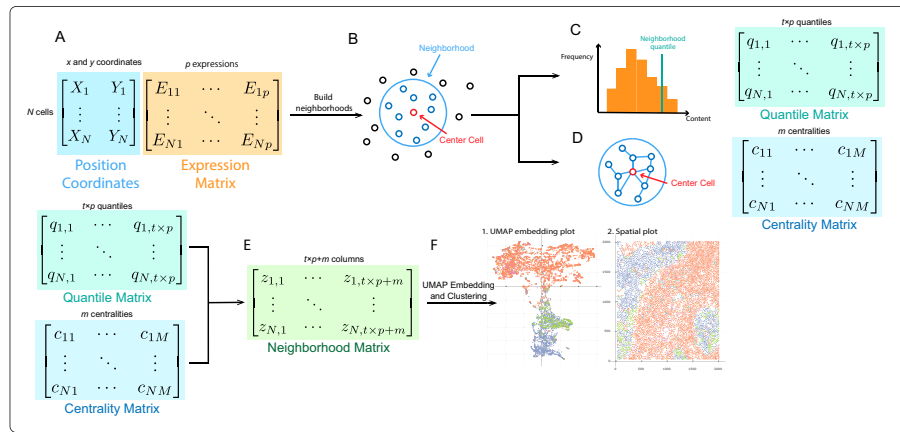
Several subtle but important details are worth noting. Before we calculate a featurization matrix, a preliminary dimensionality reduction method is needed. First, applying dimensionality reduction decreases the computational burden of downstream analysis. Computing quantiles for each feature in a high-dimensional dataset further increases the dimensionality. For example, computing 10 quantiles for each of 100 variables results in 1000 columns, which significantly increases the computational burden of embedding. Second, a statistical reason for dimensionality reduction is to reduce the noise in the original high-dimensional dataset. If the original data are effectively low-rank, then dimensionality reduction method will reduce unnecessary noise while preserving most statistical information, which is beneficial for the following embedding.

Another detail is the rescaling of the neighborhood matrix. Although the neighborhood matrix could have hundreds or even thousands of columns, there is no need to apply a preliminary dimensionality reduction to it, since all values are approximately comparable. However, it is necessary to rescale the neighborhood matrix because the ranges of different statistics vary dramatically, causing one or two variables with large variance to dominate the whole UMAP embedding. For instance, the entries in the quantile matrix were between -1.5 and 1.5 in the TNBC dataset, but for the network matrix, it is common to have some network statistics larger than 10. These network statistics would dominate the UMAP embedding if no rescaling is applied.

### Visualization design

We devised an interactive Shiny app ([Chang et al., 2015](#)) to analyze outputs from the neighborhood-based analysis, supporting visualization of microenvironment differences. In this subsection, we discuss the design and visual queries supported by the interface.

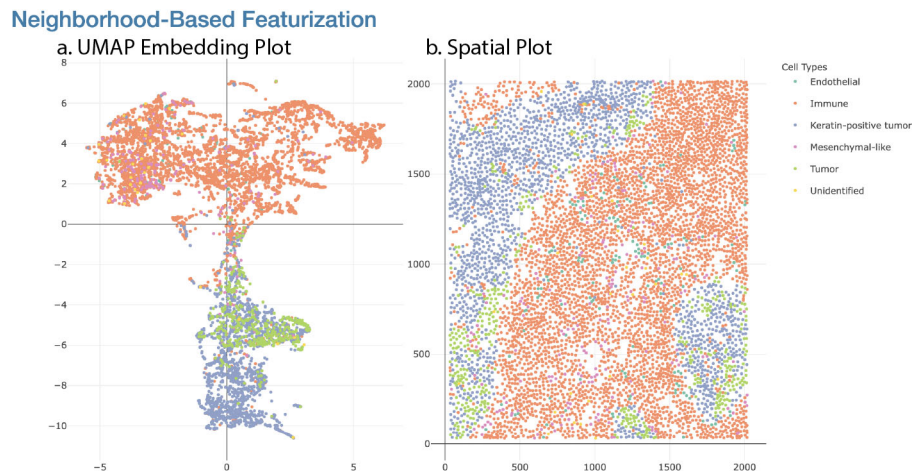




**Figure 4. The general workflow of the neighborhood-based featurization.** A) The spatial omics datasets are composed of two parts: spatial coordinates and expressions of each cell. We applied dimensionality reduction to the expression matrix to derive a reduced one on which features are derived. B) We treat each cell  $x_i$  as a center and build a neighborhood for it. There are two general ways to construct a neighborhood: using distance between spatial coordinates and using the  $K$ -nearest neighbors. In our example, we combined these methods in the following way. First, we included cells whose distance from the central cell was less than a given length. Then we only kept the nearest  $K$  cells as its neighbors. C) To derive the quantile featurization for a gene, the quantiles of the distribution of each neighborhood's expression for that gene are calculated. D) For the centrality featurization, we built a network within the neighborhood. Edges exist between two cells that are close enough. Then, we calculated centralities with respect to the center cell  $x_i$ . E) We concatenated and rescaled these derived features into what we call a neighborhood matrix. F) We applied uniform manifold approximation and projection (UMAP) to the neighborhood matrix to obtain embeddings for each cell, where we directly applied clustering algorithms. See the Example subsection below for details of the implementation.

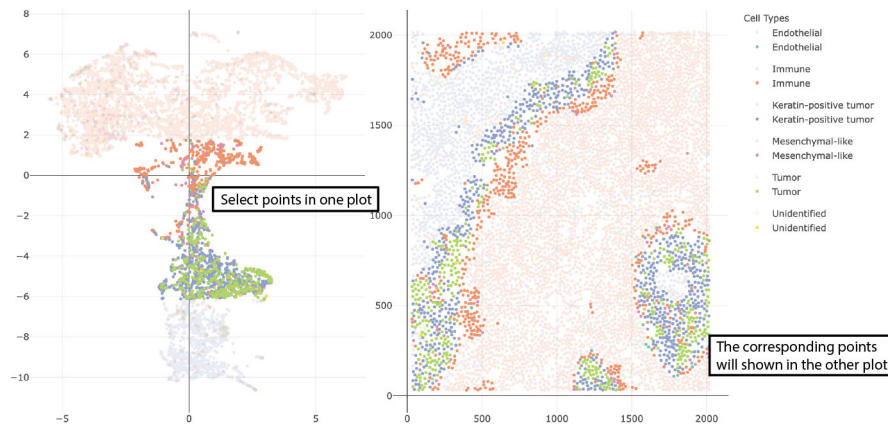
Figure 5 shows the first component of the Shiny app, the UMAP embedding and linked spatial plot. This is used to relate the low-dimensional embeddings of each cell's neighborhood features to its overall spatial context. Figure 5a is the two-dimensional UMAP embedding plot derived from the neighborhood matrix. Each point corresponds to one cell. The closer these points are, the more similar their neighborhood featurizations are. To clearly visualize the distribution of cell types, the points in Figure 5a are colored according to cell types.

Figure 5b is the spatial plot. Each point here represents a cell center, derived from the original cell polygon in the tissue section. As before, different cell types are distinguished by colors. Furthermore, the two panels in Figure 5 are dynamically linked. When points are selected in one plot through a mouse brush, the corresponding points will also be highlighted in the other plot. Figure 6 shows the highlighted points in these two plots after one such selection. We can



**Figure 5. The first component: the UMAP embedding and spatial plots.** Part (a) is the two-dimensional embedding of the neighborhood matrix, and (b) is the original spatial layout of cell types.





**Figure 6. Area selection.**

click on the legend on the sidebar to deselect these cell types so that they do not appear. **Figure 7** shows the embedding plot and scatter plot after deselecting the immune cells.

The second component of the Shiny app shows the same embeddings but colored by *K*-means cluster rather than cell type. For example, in **Figure 8**, the positions of points are still the same as in **Figure 5**, but they are clustered into five *K*-means

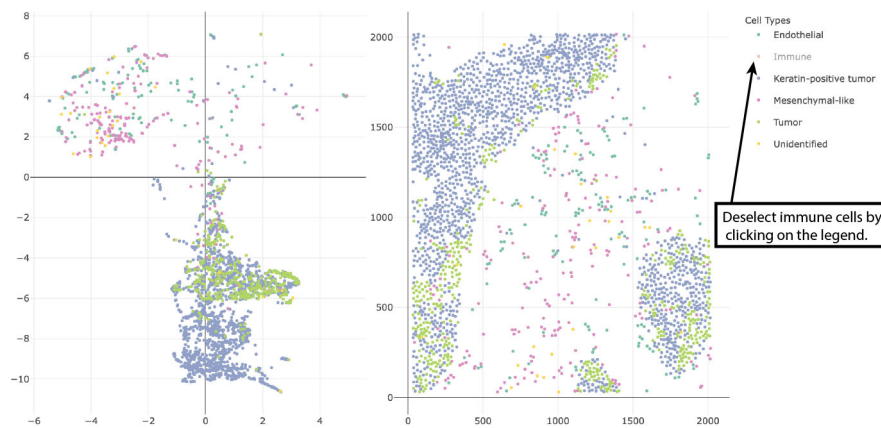


**Figure 7. Cell types can be deselected by clicking on the legend.**

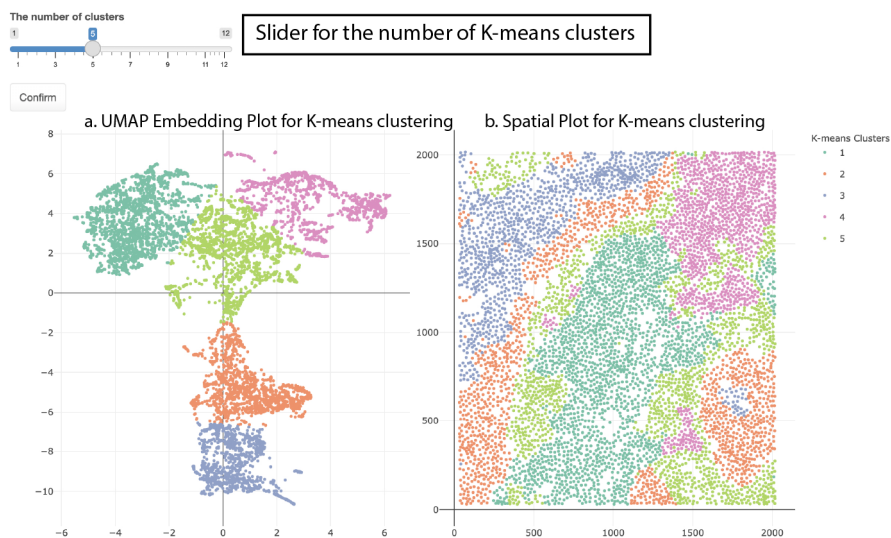


**Figure 8. The second component: UMAP embedding plot and spatial plot of *K*-means clustering.**

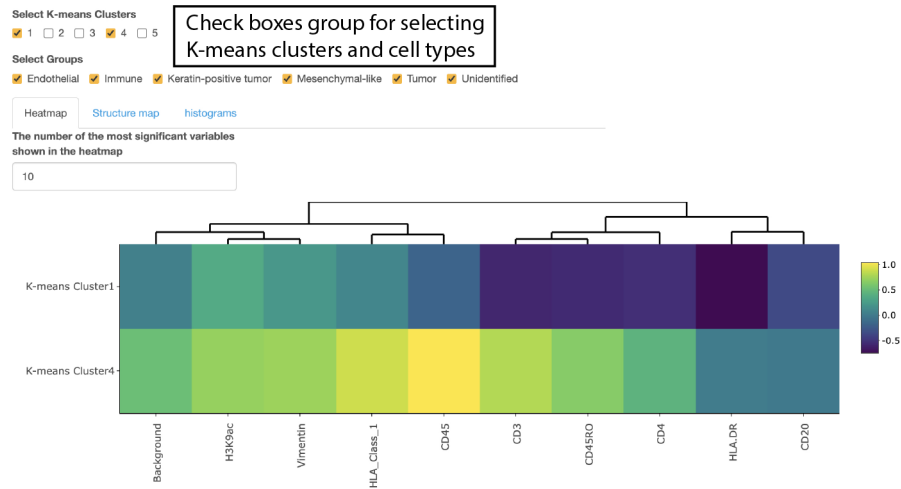


**Figure 9. The third component: Heatmap, structure plot, and histogram.** These views help describe clusters identified by *K*-means.

clusters. A slider is provided at the top of the second component in Figure 8, which is used for changing the value of *K* in the *K*-means clustering.

The third component of this Shiny app supports the comparison of expression levels across *K*-means clusters using a heatmap, structure plot, and histogram; see Figure 9. There are three tab panels with which we can switch between these three plots. Before making a further comparison, we can filter to cells of interest using the checkboxes at the top of Figure 9. Two groups of checkboxes are offered to select the cell types and *K*-means clusters to focus on. Based on the filtered cells, an expression heatmap of *K*-means clusters is provided in Figure 9. By default, it shows the top 10 most differentially expressed features across the selected clusters, based on the median of expression value in each cluster. A numeric input is offered above the heatmap – this controls the number of features appearing in the heatmap. The structure plot of the selected *K*-means clusters is provided in Figure 10, with which we can see the proportion of each cell type across every cluster. The histogram of expression is available to compare the selected feature's expression across clusters. For example, Figure 11 is the histogram of the HLA Class 1 content in Clusters 1 and 4. Note that a selection input box is offered above the histogram to change the selected feature easily.

To show the spatial distribution of a specific feature's expression, another combination of the embedding and spatial plot is provided in Figure 12. The colors of the points in Figure 12 reflect Human Leukocyte Antigen (HLA) Class 1 content.

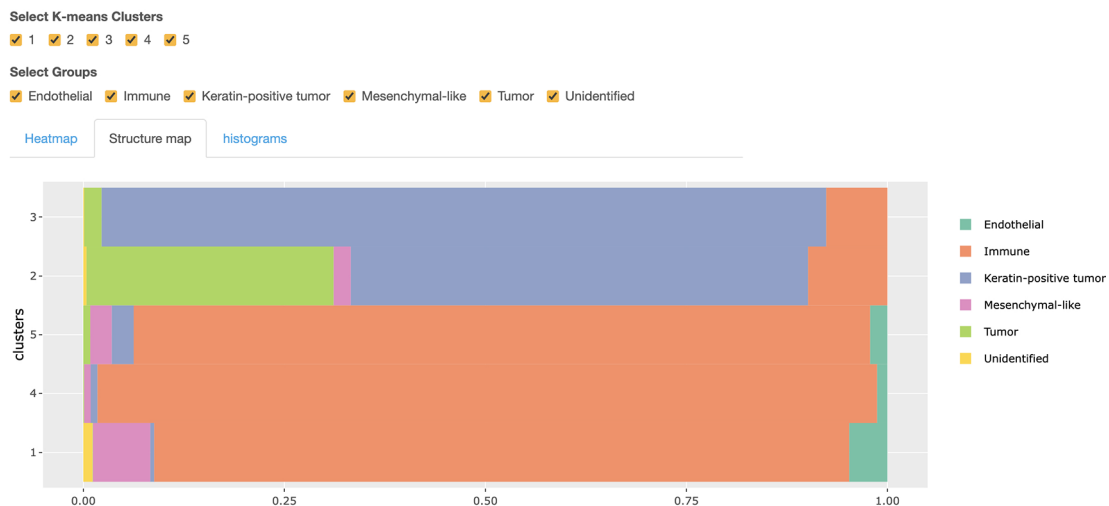


**Figure 10. Structure plot of *K*-means clusters.** The dominant cell types in each clusters are shown clearly.

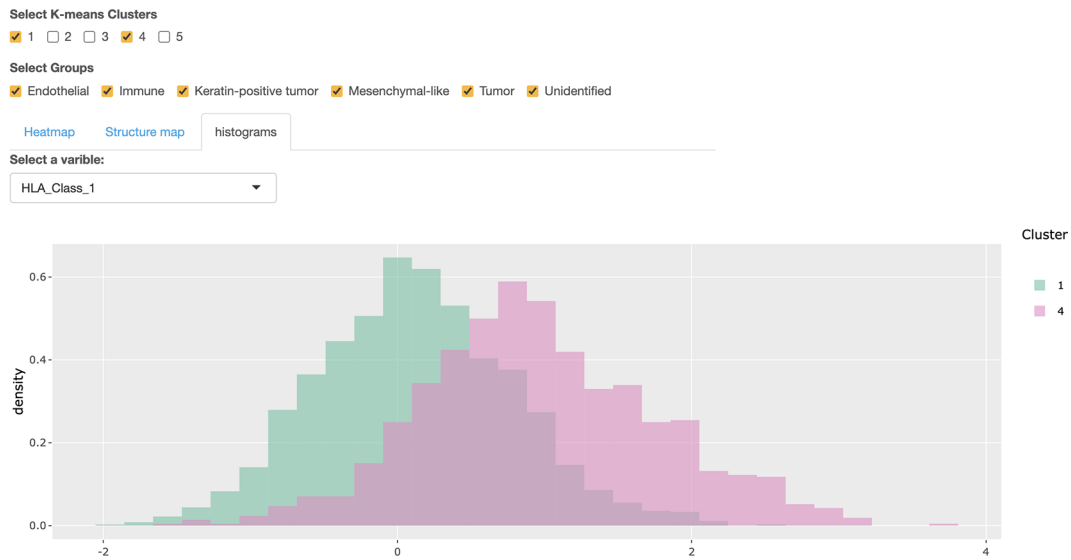


**Figure 11. Histogram of expressions among K-means clusters.** Users could select different expressions by the selection input box above the histogram.

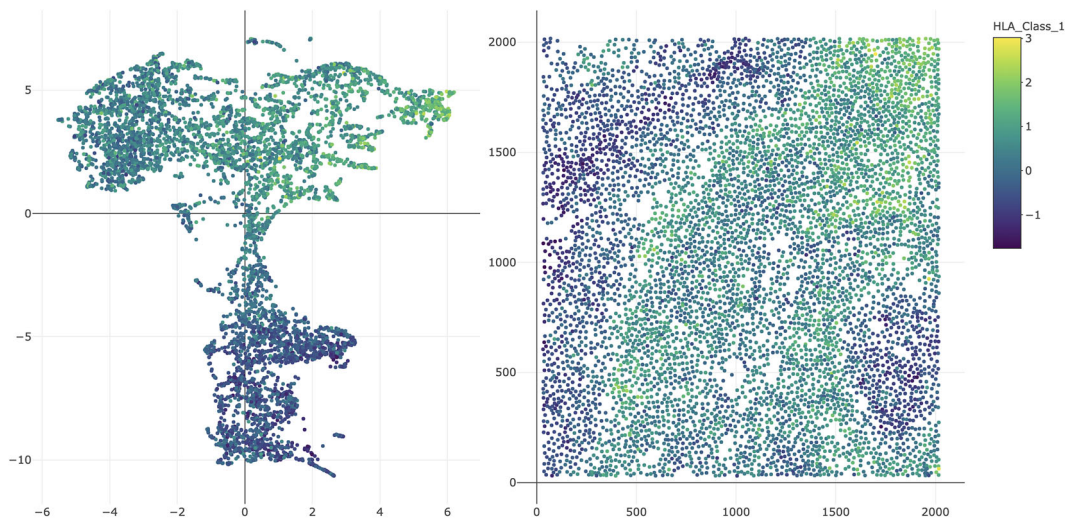


**Figure 12. Expression plot of selected cells.** Instead of coloring by cell type or K-means cluster, each cell is shaded according to the selected genomic feature.

This expression plot highlights spatial characteristics of the expression content. In this case, expression is elevated in immune cells, especially those closest to the tumor-immune boundary.

## Results

To illustrate our approach and package, we re-analyzed the Triple Negative Breast Cancer (TNBC) dataset of [Keren et al. \(2019\)](#) (*Underlying data*). To study this data, [Chen et al. \(2020\)](#) proposed Spatial-LDA, which was found to reveal novel microenvironments. Spatial-LDA models the distribution of cell types within neighborhoods but does not model protein expression directly. In contrast, our proposal considers quantitative protein measurements and network statistics within spatial neighborhoods. Here, we choose the tissue section of Patient 4, which had 6643 cells belonging to six cell types: immune cells (62.6%), keratin-positive tumor cells (25.2%), tumor cells (6.4%), mesenchymal-like cells (3.2%), endothelial cells (1.9%), and unidentified cells (0.5%). We used 41 expression variables, two-dimensional coordinates of cell centers, and cell types for further analysis.

The first step was to construct the neighborhood quantile matrix. We applied PCA to reduce the dimension of the expression matrix. We kept 19 principal components, which is the smallest number of components required to explain 90% of the variance. These components were labelled as  $PC_1, \dots, PC_{19}$ . Next, neighborhoods were defined using a radius of 60 pixels. We only include the cells among the top 40 nearest neighbors to the center cell of the neighborhood. Quantiles for each principal component were calculated based on neighborhoods. To avoid the influence of extreme values, only quantiles  $q_{0.10}, q_{0.15}, \dots, q_{0.90}$  were included. Hence, we derive a  $6643 \times 323$  quantile matrix of neighborhoods after featurization. The second step was to obtain the network matrix of the neighborhoods. We again used a radius of 60 pixels to define neighborhoods and kept only the 40 closest cells. Networks were constructed based on these neighborhoods. We linked cells whose centers were within 30 pixels of one another. Then, 29 network statistics were calculated according to the neighborhood networks; most of these network statistics were different kinds of network centralities. This resulted in a  $6643 \times 29$  neighborhood network matrix.

The third step was to combine the quantile and network matrices together into an extended neighborhood matrix. The network matrix was rescaled in this step. The result was a  $6643 \times 352$  neighborhood matrix. The final step applied dimensionality reduction and clustering to the neighborhood matrix. We applied UMAP to the neighborhood matrix to generate two-dimensional embeddings of each cell. *K*-means was applied to the UMAP embeddings to find potential clusters. These can be interpreted as microenvironments.

We used a Shiny app implemented in NBFvis to explore the result of UMAP embeddings and *K*-means clusters. Figure 13 shows the UMAP embeddings and spatial plot of the neighborhood matrix. Figure 13a gives the embeddings based on the reduction of the neighborhood matrix. The points in the embedding plot are colored according to their cell types. There are two main clusters in the embedding plot, composed primarily of immune and tumor cells, respectively. These two clusters are connected by a transition zone of a mixture of tumor and immune cells. Figure 13b is the spatial plot of the cells in the tissue section. By selecting the transition zone in the embedding plot, we found that the cells in this area are located on the boundary of immune cells, tumor cells, and keratin-positive tumor cells. This is shown in Figure 14.

*K*-means clustering applied to the UMAP embeddings suggests potential microenvironments. Figure 15 shows clustering results with  $K = 5$ . The clusters are distinguished by their colors. In the embedding plot Figure 15a, the embeddings are divided into five clusters, and the corresponding locations of these clusters are shown in the spatial plot Figure 15b. One finding of note is that the clusters in the embedding space were spatially consistent.

In Figure 15b, two microenvironments were found among the tumor cells and keratin-positive tumor cells, Cluster 3 in the inner part of the tumor cell groups and Cluster 4 close to the boundary of immune cells. This mirrors the findings of Chen et al. (2020). Another finding was a special immune cell microenvironment, Cluster 2, lying on the boundary of immune cells, tumor cells, and keratin-positive tumor cells. This microenvironment was distinguished from the immune microenvironment in the inner part of immune cell groups, which is Cluster 5 in Figure 15b. Notice that

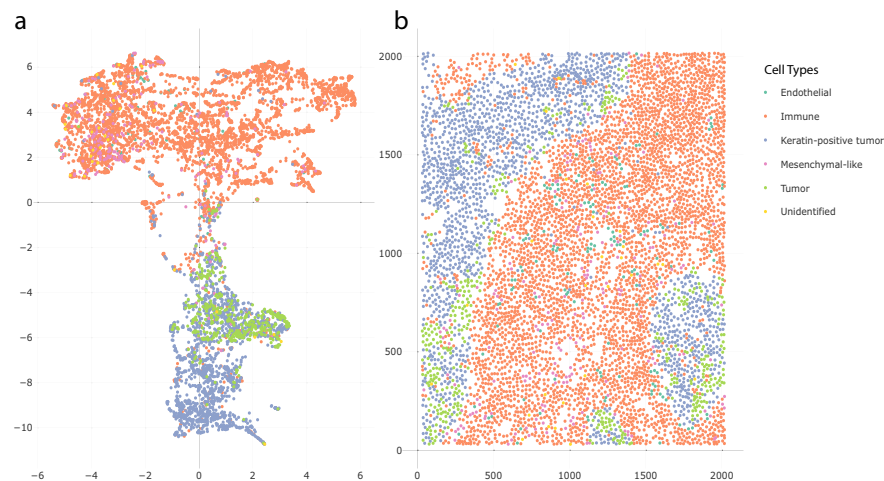


**Figure 13. UMAP embedding and spatial plots using neighborhood-based featurization.** Panel (a) is the UMAP embedding plot colored in cell types. Panel (b) is the spatial plot of the real positions of cell centers. We observe a transition zone between clusters of tumor cells and immune cells in part (a).



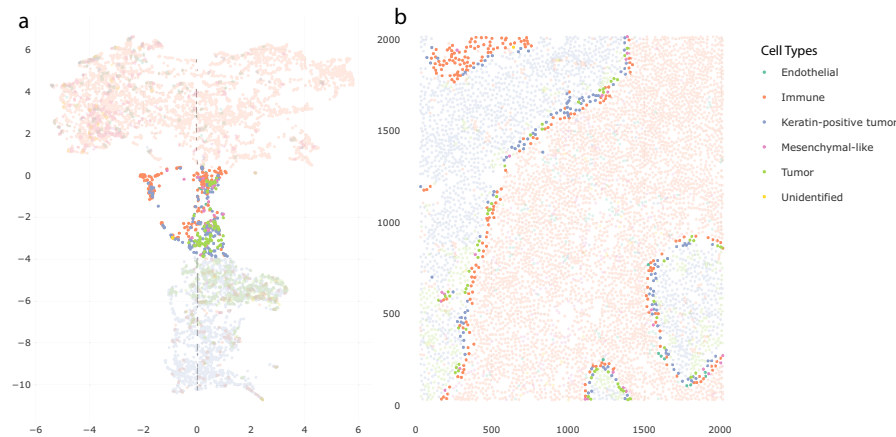


**Figure 14. Transition zone in the UMAP embedding and spatial plots.** The corresponding cells whose embeddings are in the transition zone in panel (a) are located close to the tumor-immune boundary in panel (b).

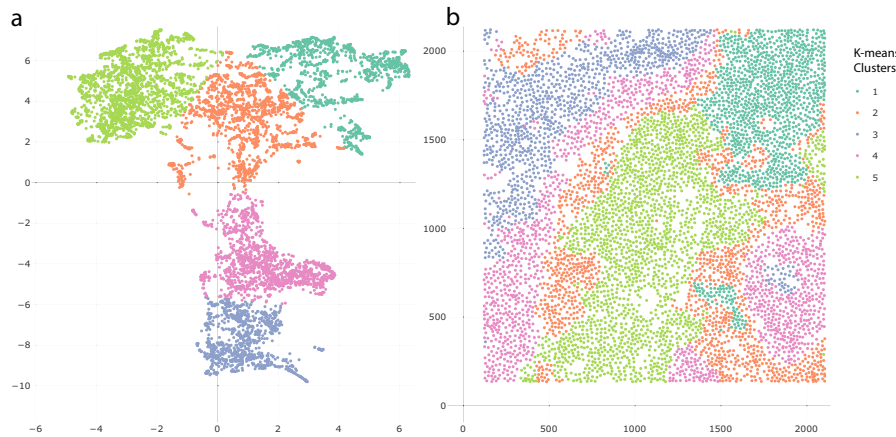


**Figure 15. K-means embedding and spatial plots with  $K = 5$ .** Clusters in panel (b) are spatially consistent. There are two special clusters on the tumor-immune boundary, whose embeddings are in the transition zone in panel (a).

Clusters 4 and 5, which are the microenvironments close to the tumor-immune boundary, are in the transition zone in the UMAP embedding plot in [Figure 14](#). Moreover, another microenvironment, Cluster 3, was found in the top-left corner of [Figure 15b](#), separate from the previous two immune microenvironments, Clusters 2 and 5.

Next, we explored the differences between these microenvironments by studying their expression patterns. [Figure 16](#) is the heatmap of the inner and boundary immune microenvironments, which are Clusters 2 and 5 in the [Figure 15b](#), respectively. The heatmap shows the top 10 most differentially expressed proteins between these two clusters, determined by the differences between medians of expressions in each group. We chose the two most differentially expressed proteins, CD45 and CD45RO, for further exploration. The histograms in [Figure 17](#) show the contents of CD45 across these two microenvironments. The inner immune microenvironment has a right-skewed distribution of CD45, indicating that many cells in this microenvironment have a low content of CD45. In contrast, the distribution of CD45 in the boundary immune microenvironment was significantly higher than that in the inner immune microenvironment. [Figure 18](#) is the expression plot of CD45, this confirms that cells along the tumor-immune boundary had elevated CD45.

Checking the histogram and spatial expression of CD45RO in the inner and boundary immune microenvironments, we arrived at similar conclusions. [Figure 19](#) is the histogram of these two microenvironments. The histogram for the inner immune microenvironments has a peak near the minimal value, which does not appear on the histogram of the boundary immune microenvironments. It shows that there were lower contents of CD45RO in the inner immune microenvironment but higher contents of CD45RO. [Figure 20](#) also shows that there was a lighter boundary on the tumor-immune cells, highlighting this microenvironment.

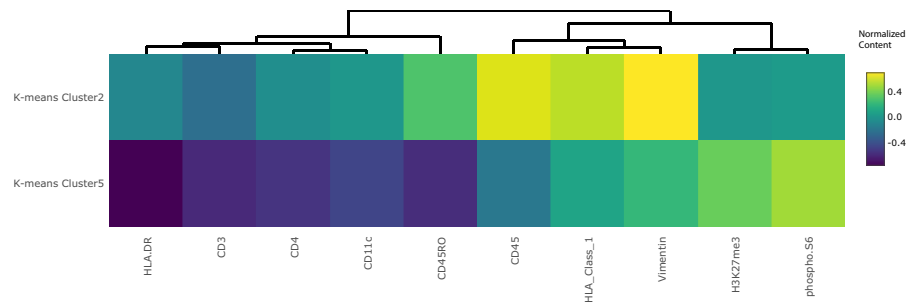


**Figure 16. Heatmap of expressions in Cluster 2 and 5.** Cluster 2 is on the tumor-immune boundary and Cluster 5 is in the inner part of immune cell groups. The most obvious difference in expressions between these two clusters are CD45 and CD45RO. Cluster 5 had significantly lower CD45 and CD45RO content than Cluster 2.

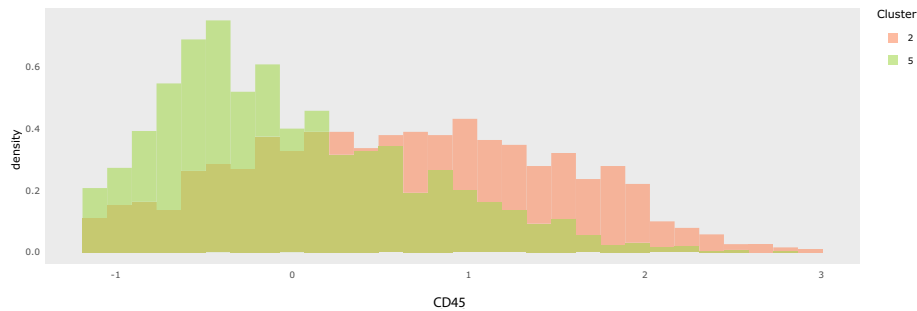


**Figure 17. Histograms of CD45 across Clusters 2 and 5, highlighting elevated CD45 levels in immune cells closer to the tumor-immune boundary.** Histograms for different features can be selected using the interface, and the choice can be guided by a heatmap like in Figure 16.

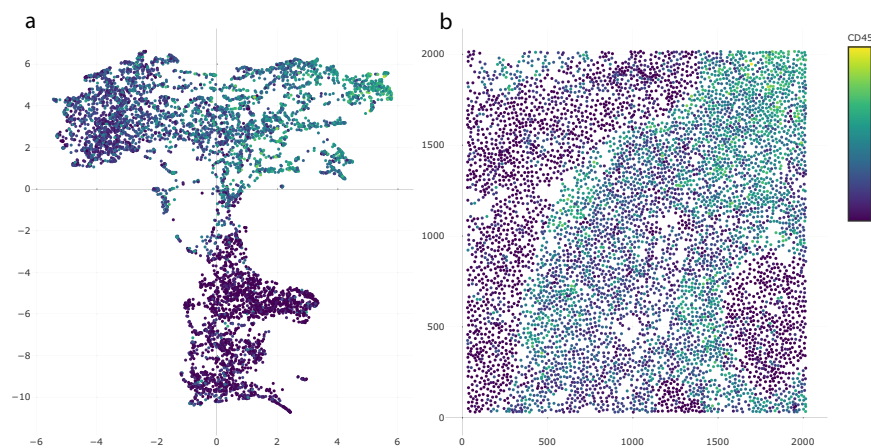


**Figure 18. UMAP embedding and spatial plots shaded in according to measured CD45.** The existence of brighter cells near the tumor-immune boundary is consistent with Figures 16 and 17. This view also reveals elevated CD45 in the top-right region, corresponding to Cluster 3.

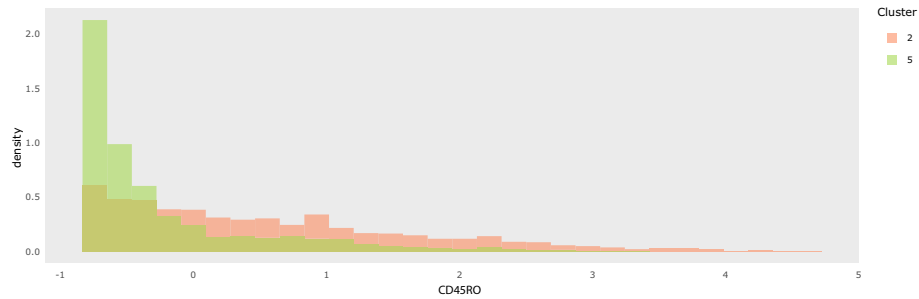


**Figure 19.** The analog of [Figure 17](#) for CD45RO, another marker found to be differentially expressed across Clusters 2 and 5. In contrast to CD45, the distribution in both clusters is strongly right-skewed, even after the preprocessing applied by [Keren et al. \(2019\)](#).

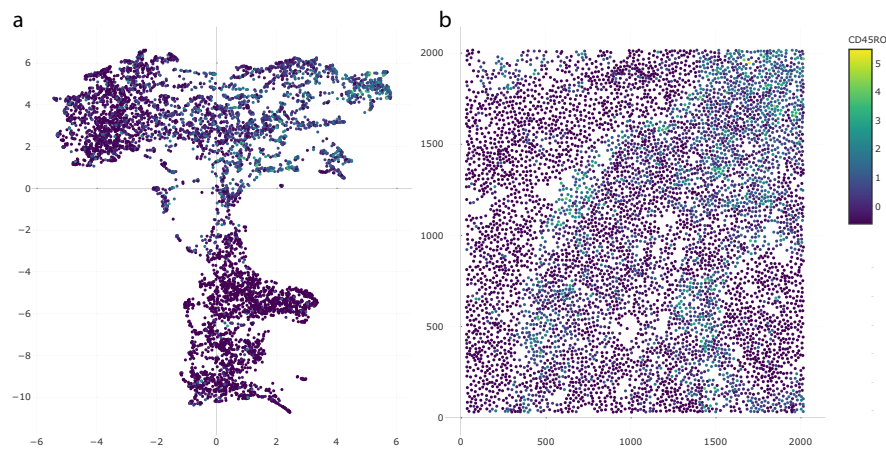


**Figure 20.** The analog of [Figure 18](#) for CD45RO. This marker's spatial expression structure is similar to that for CD45. The fact that more cells are shaded darkly reflects the right skew observed in the histograms in [Figure 19](#).

### Cell-level approach

We also used the visualization tool to show the UMAP embedding and clustering results when directly applied to the original cell-level protein expression matrix. We used the same preprocessing as [Keren et al. \(2019\)](#). This serves as a reference point against which to compare the proposed neighborhood-based featurization.

[Figure 21](#) gives the UMAP embedding and spatial plot using the cell-level approach. We found two clusters in the [Figure 21a](#), one mainly made up of immune and one of tumor cells, respectively. The result was similar to the simulation, where UMAP embeddings were dominated by the differences between cell types and microenvironments were hardly distinguishable.

[Figure 22](#) shows the clustering results after  $K$ -means clustering with  $K = 5$ . The clustered microenvironments were mixed with each other; in particular, it was difficult to distinguish a tumor-immune boundary microenvironment. [Figure 23](#) compares the clustered spatial plots based on the cell-level and neighborhood-based approaches. In [Figure 23a](#), the cells in Region 1 were a mixture of three microenvironments derived from the cell-level approach. It was difficult to identify which microenvironment this region belonged to. Although Region 2 of [Figure 23a](#) was mainly composed of Cluster 3, there were cells from Clusters 4 and 5 distributed throughout. Though in principle it is possible to distinguish microenvironments based on particular mixture patterns across cell types, doing so requires much more effort than examining the neighborhood-based representation.

Compared with the cell-level approach, the neighborhood-based featurization has a noticeably clearer clustering result. In Region 1 of [Figure 23b](#), the cells in the boundary of tumor cells are spatially consistent according to their own cell types. Further, in Region 2 of [Figure 23b](#), we observe a dominant microenvironment without needing to parse mixed patterns of cell types.



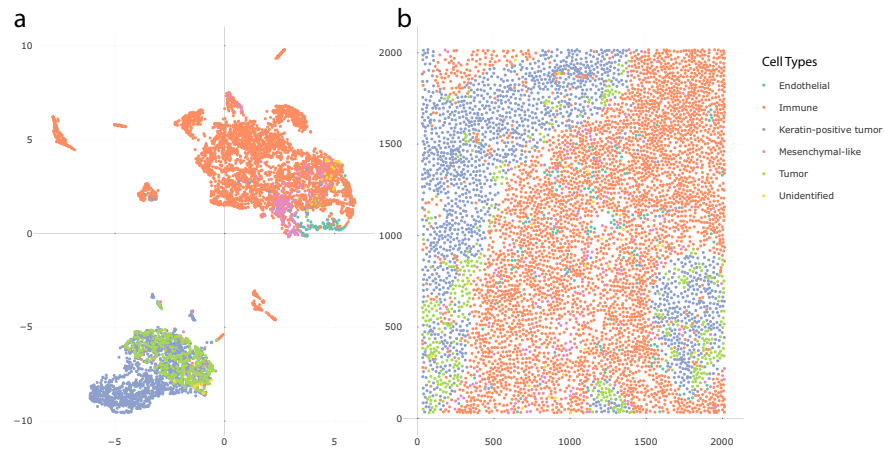


**Figure 21.** The UMAP embedding and spatial plots obtained without neighborhood features. Cells are shaded by cell type. Compare with Figure 13.

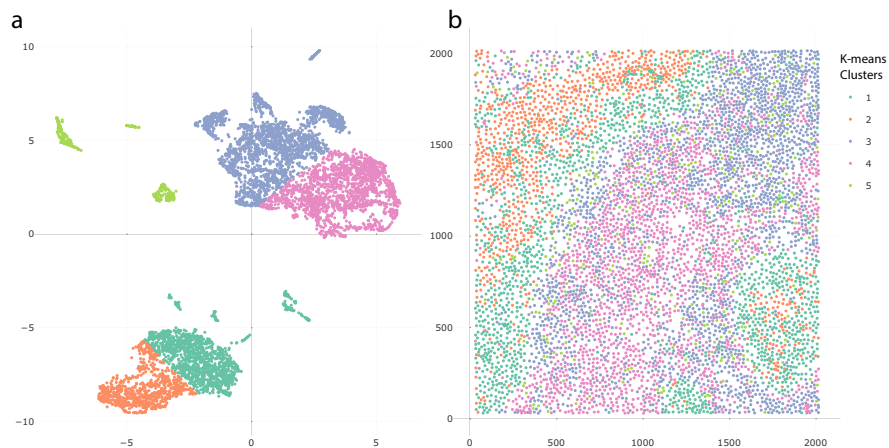


**Figure 22.** A version of Figure 21 where cells are shaded by *K*-means clusters found in the embedding on the left. Sub-cell type variation in the embedding plot does not correspond to spatially meaningful microenvironments. Compare with Figure 15.

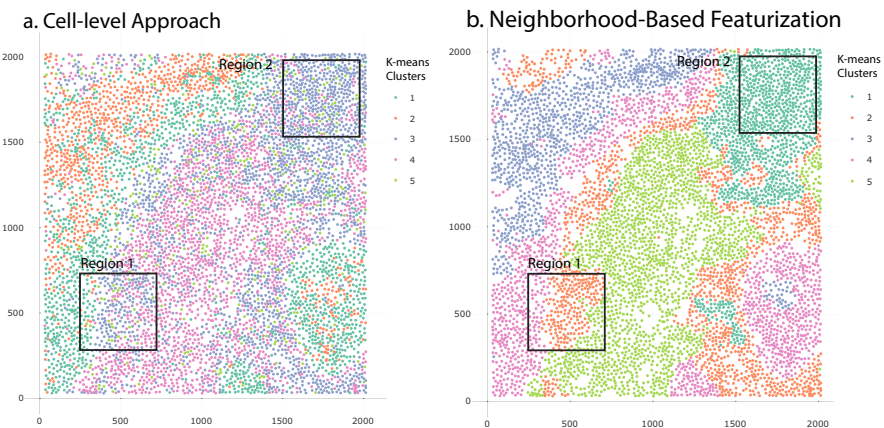


**Figure 23.** A direct comparison of the spatial plots from Figures 15 and 22. Microenvironments with similar expression patterns (and stable cell type mixtures) are enclosed in black boxes. Microenvironments are more clearly visible when using neighborhood-based featurization.

Overall, the neighborhood-based featurization provides representations with better spatial consistency, simplifying the discovery of microenvironments.

### Package

We next summarize how to use NBFvis to implement the proposed workflow. We first loaded the packages and dataset we need. The dataset `patient4` is a  $6643 \times 59$  data frame of all cells in the tissue section of Patient 4 in the TNBC data (Keren et al., 2019). We added two columns named `x_center` and `y_center`, which are the coordinates of the calculated cell centers from the spatial raster data.

```
library (NBFvis)
library (dplyr)
data (patient4)
```

We selected 41 variables from `dsDNA` to HLA Class 1, most of which are proteins and cell type markers. The `quantile_matrix` function generates the quantile matrix from each cell's neighborhood.

```
Quantiles_patient4 <- quantiles_matrix(
  data = patient4 %>% select (dsDNA:HLA_Class_1),
  coordinate = patient4 %>% select(x_center,y_center),
  index = patient4$index,
  NN = 40,
  distance = 60,
  min_percentile = 0.1,
  max_percentile = 0.9,
  quantile_number = 17,
  method = pca_)
```

The function `network_matrix` first builds the network inside the neighborhood and then calculates the corresponding network statistics using the argument given by `fun`. In this example, we used the function `centralities`, also exported by our package.

```
centrality_patient4 <- network_matrix(
  coordinate = patient4 %>% select (ends_with("_center")),
  index = patient4$index,
  radius = 60,
  NN = 40,
  edge = 30,
  fun = centralities,
  length_output = 29,
  name_output = NULL)
```

The scales of these two matrices are not the same, which means rescaling is needed. Here we removed `Column`, `index` and `n_neighborhood` in the quantile matrix so that all the columns left were quantile and network variables. Normalization and centering were applied to the centralities matrix so that they had a similar scale to the quantile matrix. We then combined the quantile matrix and the rescaled network matrix to construct an extended featurization matrix, which we called the neighborhood matrix earlier.

```
neighborhood_info_patient4 <- cbind(
  Quantiles_patient4 %>% select(-index, -n_neighbor),
  scale (centrality_patient4 %>% select(-index)))
```

The final step was to input the neighborhood matrix, the cell dataset `patient4`, and the names of the variable of interest in the function `NBFvis`. This returned an interactive Shiny app that was the source of figures in the Results section,

```
NBF_vis(
  matrix = neighborhood_info_patient4,
  origin_data = patient4,
  var_names = colnames (patient4)[ 17:57] )
```

## Discussion

We have presented a method for visualizing spatial omics datasets that integrates dimensionality reduction methods like UMAP with neighborhood-based featurization based on quantiles and network properties. According to the results of our simulation, dimensionality reduction based on genomic features alone has difficulty identifying microenvironments because the associated embeddings are dominated by differences in expression patterns across cell types. Also, *K*-means clustering on the UMAP embeddings from this approach results in spatially inconsistent clusters, making it difficult to identify potential microenvironments. In contrast, our approach, though simple to implement, is able to avoid these problems by leveraging neighborhood information of cells. After combining neighborhood-based statistics like quantiles and centralities, we can detect microenvironments with mixed cell types, paralleling our simulation results. Furthermore, spatially consistent *K*-means clusters can be derived, supporting discovery of microenvironments.

We applied our methodology to the spatial omics dataset of (Keren et al., 2019) and found five spatially continuous microenvironments in the cells' spatial plot. We compared this result with the analogous approach based on cell-level data and found that it is more difficult to identify meaningful microenvironments without an initial featurization step.

One advantage of our methodology is that the choice of neighborhood-based featurization is flexible. In our example, we used neighborhood quantiles of principal components and network statistics to build the neighborhood matrix for UMAP. These statistics could be replaced by other neighborhood-based statistics like cell-type diversity or local modularity. Also, the embedding and clustering methods are not fixed. We could use alternative dimensionality reduction methods like *t*-distributed stochastic neighbor embedding (*t*-SNE) and PCA or clustering methods like spectral clustering depending on the problem structure.

There are several avenues to develop this work. First, we treated the nodes in the neighborhood networks identically, ignoring their cell types. This is convenient for the computation of network statistics, but the information is nonetheless lost. To address this, it may be possible to build neighborhood networks with different node types and compute corresponding network statistics. A second question is how to combine matrices. Our featurization is based on matrices from two groups of statistics (quantiles and network statistics), and their variances and interpretation could be quite different according to their groups. Is there a more principled approach to scaling and combining these measures into a single featurization? One possible solution could be multiple factor analysis, which distinguishes between groups of statistics (Pagès, 2014). Thirdly, we used *K*-means clustering in our methodology, which is a common choice but far from the best clustering algorithm for low-dimensional embeddings. *K*-means clustering is sensitive to outliers in the embedding plot and assumes spherical clusters, making it potentially unreliable. Spectral clustering could be a potential improvement because it is more sensitive to the gradient structures in the UMAP embeddings.

## Data availability

### Underlying data

The TNBC dataset of Keren et al. (2019) can be downloaded from <https://www.angelolab.com/mibi-data>.

### Extended data

Analysis code available from: <https://github.com/XTH1114/NBFvis>

Archived analysis code as at time of publication: DOI: [10.5281/zenodo.6639613](https://doi.org/10.5281/zenodo.6639613)

License: GNU General Public License

## Acknowledgements

We would like to express our gratitude to all the members of our group, who provided us with precious suggestions for the modification of our methodology and the Shiny app. In particular, we thank MinXing Zheng for suggestions on the choices of network statistics and Xinran Miao and Hanying Jiang for help improving the user interface of our Shiny app.

## References

Burgess DJ: **Spatial transcriptomics coming of age.** *Nat. Rev. Genet.* 2019; **20**(6): 317–317.  
[PubMed Abstract](#) | [Publisher Full Text](#)

Butts CT: *sna: Tools for Social Network Analysis.* 2020. R package version 2.6.  
 Tables.  
[Reference Source](#)

Chang W, Cheng J, Allaire JJ, *et al.*: **Package 'shiny'**. 2015.

[Reference Source](#)

Chen Z, Soifer I, Hilton H, *et al.*: **Modeling multiplexed images with spatial-lda reveals novel tissue microenvironments**. *J. Comput. Biol.* 2020; **27**(8): 1204–1218.

[PubMed Abstract](#) | [Publisher Full Text](#)

Csardi G, Nepusz T: **The igraph software package for complex network research**. *Interjournal, Complex Systems*. 2006; 1695.

[Reference Source](#)

Dries R, Chen J, Del Rossi N, *et al.*: **Advances in spatial transcriptomic data analysis**. *Genome Res.* 2021a; **31**(10): 1706–1718.

[PubMed Abstract](#) | [Publisher Full Text](#)

Dries R, Zhu Q, Dong R, *et al.*: **Giotto: a toolbox for integrative analysis and visualization of spatial expression data**. *Genome Biol.* 2021b; **22**(1): 1–31.

Hsu L, Culhane A: **Tumor spatial autocorrelation and clinical prognosis**. 2020.

[Reference Source](#)

Jalili M: *centiserve: Find Graph Centrality Indices*. 2017. R package version 1.0.0.

[Reference Source](#)

Keren L, Bosse M, Thompson S, *et al.*: **Mibi-tof: A multiplexed imaging platform relates cellular phenotypes and tissue structure**. *Sci. Adv.*

2019; **5**(10): eaax5851.

[PubMed Abstract](#) | [Publisher Full Text](#)

McInnes L, Healy J, Melville J: **Umap: Uniform manifold approximation and projection for dimension reduction**. *arXiv preprint arXiv:1802.03426*. 2018.

Nawy T: **Spatial transcriptomics**. *Nat. Methods*. 2018; **15**(1): 30–30.

[Publisher Full Text](#)

Pagès J: *Multiple factor analysis by example using R*. CRC Press; 2014.

Rao A, Barkley D, França GS, *et al.*: **Exploring tissue architecture using spatial transcriptomics**. *Nature*. 2021; **596**(7871): 211–220.

[PubMed Abstract](#) | [Publisher Full Text](#)

Sun S, Zhu J, Zhou X: **Statistical analysis of spatial expression patterns for spatially resolved transcriptomic studies**. *Nat. Methods*. 2020; **17**(2): 193–200.

[PubMed Abstract](#) | [Publisher Full Text](#)

XTH1114:Sankaran K: **Xth1114/nbfvis: v1.0.1**. June 2022.

[Publisher Full Text](#)

Yoozuf N, Navarro JF, Salmén F, *et al.*: **Identification and transfer of spatial transcriptomics signatures for cancer diagnosis**. *Breast Cancer Res.* 2020; **22**(1): 1–10.

[Publisher Full Text](#)

Zhu J, Sabatti C: **Integrative spatial single-cell analysis with graph-based feature learning**. *bioRxiv*. 2020.

# Open Peer Review

Current Peer Review Status: ? ?

Version 1

Reviewer Report 02 September 2024

<https://doi.org/10.5256/f1000research.134059.r250359>

© 2024 Ospina O. This is an open access peer review report distributed under the terms of the [Creative Commons Attribution License](#), which permits unrestricted use, distribution, and reproduction in any medium, provided the original work is properly cited.



**Oscar Ospina**

Moffitt Cancer Center, Tampa, Florida, USA

The manuscript “Interactive visualization of spatial omics neighborhoods” presents a novel and “out of the box” proposal to define cellular neighborhoods from spatial proteomics (and potentially) transcriptomics data. The method is a very interesting approach to the spatial analysis of data modalities that are becoming increasingly popular in the literature. I appreciate not only the statistical framework (called NBFvis) behind the model, but also that the authors made efforts to make the pipeline partially interactive.

Despite the high current relevance of the data types involved and the novel approach devised by the authors, I consider some major points should be addressed:

Major comments:

- I think it's critical that the method is tested on various tissue types. The users presented the results of running NBFvis on a TNBC sample. However, not all cancer tissues (or even healthy tissues) have a clear structure and compartments. Often, one can find tissue samples where the cells are highly intermixed, and defining microenvironments becomes very challenging. I also think it's important that NBFvis is tested on data from other technologies, such as spatial transcriptomics.
- It is equally important that the method is benchmarked against other tissue domain/microenvironment methods. For example, SpaGCN for spatial transcriptomics, or MILWRM for proteomics/transcriptomics. To mention the first two that came to my mind. The field is saturated with methods to achieve similar goals to what NBFvis does, and comparing to others can help the reader ponder the advantages over other methods.
- Following on the previous point, the authors mentioned SPARK in the “Background” section. But if NBFvis is a microenvironment detection method, it makes more sense to cite other spatial domain/microenvironment detection methods. Spatial-LDA is, of course, one of them, but many others are available, especially if NBFvis is proposed as a solution for spatial transcriptomics.
- I appreciate the efforts to test NBFvis on a simulated data set. However, I think the simulated data is too simplistic for the intended application. It is true that some older

spatial proteomics data only offers a few markers, but this is rapidly changing, and many technologies offer many more markers (10s-100s). Simulating only five proteins seems overly simplistic. In addition, the almost clear-cut differences between cell types are seldom encountered in real data sets. Defining cell types is, in itself, a challenging task in large part because the information from the markers does not provide the categorized levels one would expect due to either technical noise or biology itself. This is especially true for spatial transcriptomics.

- Another important thing about the simulation performed is that it was unclear what the level of feature dropout was. In spatial omics data, it is very common for a large percentage of the data to consist of zeroes. This has tremendous implications when defining cell types or neighborhoods.
- It seems that the selection of a radius can significantly impact the results. I suspect the choice of a radius size must be largely driven by the knowledge of the cell biology of the specific tissue being studied or even the research question. However, the authors could have tested several radius sizes to inform the readers about the effects of radius selection.
- Similarly, selecting the number of PCs might be important. It seems NBFvis does not allow the user to specify the number of PCs. That 19 PCs explained 90% of the variation for the TNBC data does not imply that 19 PCs will also explain that amount of variance for other data sets.
- Throughout the manuscript, it seems the authors are arguing against identifying clusters of cell types instead of “microenvironments”. Yet, in many cases, researchers indeed seek to phenotype their data sets to the cell level instead of the “microenvironment” level. This should be stated appropriately at the beginning of the manuscript, clarifying that NBFvis is a solution to the specific problem of tissue domain/microenvironment detection and not necessarily to cell phenotyping.
- What is the biological meaning of the centrality metrics? This is not addressed. Perhaps some testing of the method using several combinations of these parameters can provide a glimpse into this. Also, allowing the users to select which centrality metrics to incorporate in the embeddings may (or may not) be helpful.

#### Minor comments:

- In the abstract, I suggest changing “We designed quantile and network-based spatial features...” to “We developed a method that uses quantile and network-based spatial features...”.
- “... in the R package NBFvis, available on GitHub.” The link to GitHub repo is not working.
- It looks like the “single-cell matrix” and “expression matrix” terms are used interchangeably. I suggest uniformizing the use of the terms throughout the manuscript.
- The column names in the output of “network\_matrix” are “statistics1”, “statistics2”... etc. Would it be more informative to conserve the actual name of the network metric?

#### Suggestions for the code:

- I suggest adding the dependencies in the DESCRIPTION file. I had to re-try the installation several times as I had to install several dependencies. These are some of the unspecified dependencies: expm, shinythemes, centiserve, heatmaply, sna.

### Is the rationale for developing the new method (or application) clearly explained?

Partly

### Is the description of the method technically sound?

Partly

**Are sufficient details provided to allow replication of the method development and its use by others?**

Yes

**If any results are presented, are all the source data underlying the results available to ensure full reproducibility?**

Yes

**Are the conclusions about the method and its performance adequately supported by the findings presented in the article?**

Partly

**Competing Interests:** No competing interests were disclosed.

**Reviewer Expertise:** Spatial biology, bioinformatics, oncology

**I confirm that I have read this submission and believe that I have an appropriate level of expertise to confirm that it is of an acceptable scientific standard, however I have significant reservations, as outlined above.**

Reviewer Report 02 April 2024

<https://doi.org/10.5256/f1000research.134059.r255790>

© 2024 Peng G et al. This is an open access peer review report distributed under the terms of the [Creative Commons Attribution License](#), which permits unrestricted use, distribution, and reproduction in any medium, provided the original work is properly cited.



**Guangdun Peng**

University of Chinese Academy of Sciences , Center for Cell Lineage and Atlas, Bioland Laboratory , Guangdong Provincial Key Laboratory of Stem Cell and Regenerative Medicine , Guangzhou Institutes of Biomedicine and Health, Guangzhou, China

**Miao Zhu**

GIBH, CAS, Guangzhou, China

The manuscript entitled “Interactive visualization of spatial omics neighborhoods”, Xinghua et al. developed a new interactive tool named NBFvis for computing and visualizing low-dimensional representation of spatial protein omics data that incorporates spatial local neighborhood information. The authors attempt to address the challenge in spatial omics to learn the content-awareness low-dimensional representations for precise microenvironment identification. Like Spatial-LDA, the method learned the local neighbors’ protein expression and network statistics to create a neighbor-aware low-dimensional representation and then utilized this representation in downstream UMAP embedding and clustering. The authors validated their method by applying it to simulation data and real TNBC spatial MIBI-TOF data. They also provided a Shiny application for



interactive explode of low-dimensional representations.

The main limitation is the lack of reasonable comparisons to validate this method. The authors demonstrated the learned low-dimensional embeddings can be used to precisely identify the microenvironment on protein profile simulation data and TNBC spatial MIBI-TOF data, further showcasing the validity or accuracy of using this low-dimensional embedding to identify the microenvironment would be valuable. Perhaps comparing the accuracy of classifiers, like SVM, trained on different low-dimensional representations to distinguish manually annotated microenvironments can help demonstrate this. Secondly, the content-aware low-dimensional representations were constructed by concatenating two matrices: a quantile matrix based on neighbor protein expression and a centrality matrix based on network statistics. It is worth knowing which matrix or which network features are more crucial in identifying the microenvironment, maybe this can help to provide biological interpretations of those identified microenvironments.

Minor concerns:

1. The title "Interactive visualization of spatial omics neighborhoods" may not be suitable as the authors only validated their method on spatial protein omics data in this manuscript.
2. In the assumption of the simulated dataset, please explain more about the coefficient in the covariance matrix of the multivariate normal distribution model.
3. How is the study compared to other methods on simulated data or simulating microenvironment? e.g. SOTIP and scDesign3, more benchmarking work (tools and dataset) would be useful.
4. Is the finding that CD45 is important for tumor microenvironment supported by experiment or literature?
5. To improve the readability of the study, I would encourage the authors to reorganize the figures and merge the figures which explained similar conclusions.

**Is the rationale for developing the new method (or application) clearly explained?**

Partly

**Is the description of the method technically sound?**

Partly

**Are sufficient details provided to allow replication of the method development and its use by others?**

Yes

**If any results are presented, are all the source data underlying the results available to ensure full reproducibility?**

Yes

**Are the conclusions about the method and its performance adequately supported by the findings presented in the article?**

Partly

**Competing Interests:** No competing interests were disclosed.

**Reviewer Expertise:** technical and analytical method development for spatial multiomics;

developmental biology; stem cell biology

**We confirm that we have read this submission and believe that we have an appropriate level of expertise to confirm that it is of an acceptable scientific standard, however we have significant reservations, as outlined above.**

---

The benefits of publishing with F1000Research:

- Your article is published within days, with no editorial bias
- You can publish traditional articles, null/negative results, case reports, data notes and more
- The peer review process is transparent and collaborative
- Your article is indexed in PubMed after passing peer review
- Dedicated customer support at every stage

For pre-submission enquiries, contact [research@f1000.com](mailto:research@f1000.com)

**F1000Research**